International Journal of Thermal Sciences 61 (2012) 28–37

Contents lists available at SciVerse ScienceDirect

International Journal of Thermal Sciences

journal homepage: www.elsevier.com/locate/ijts

Thermo-hydraulic characteristics of laminar flow in an enhanced tube with conical strip inserts

Yonghua You, Aiwu Fan*, Wei Liu, Suyi Huang

School of Energy and Power Engineering, Huazhong University of Science and Technology, 1037 Luoyu Road, Wuhan 430074, China

ARTICLE INFO

Article history:
Received 4 February 2012
Received in revised form
27 June 2012
Accepted 27 June 2012
Available online 28 July 2012

Keywords:
Thermal augmentation
Flow resistance
Laminar flow
Conical strip insert
Thermo-hydraulic performance
Numerical simulation

ABSTRACT

Our previous study has demonstrated that the conical strip inserts have a good thermo-hydraulic performance in the tubular turbulent flow regime. This paper investigates its thermo-hydraulic performance of laminar flow numerically. Effects of some geometrical parameters are studied. Computation results show that the average Nusselt number of enhanced tube is augmented by 3.70–5.51 times (average $Nu = 16.15–24.05$), while the average friction factor increases by 5.31–14.77 times (average $f = 0.59–1.51$) those of plain tube. The values of performance evaluation criterion (PEC) range between 1.17 and 2.97. Numerical results indicate that larger strip size (characterized by a geometry angle), smaller strip-wall gap and smaller strip pitch can effectively enhance the heat transfer rate, but also increase the flow resistance. The impact of slant angle depends on the magnitude of Reynolds number. Moreover, it is shown that the Nusselt number and friction factor are sensitive to the geometry angle, while the most sensitive factor of PEC value is the strip pitch. Relatively high PEC value is obtained at a parameter combination with small slant angle, strip-wall gap, strip pitch, and moderate geometry angle ($\alpha = 30^\circ$, $\delta/D = 0.10$, $s/D = 1.5$, $\beta = 60^\circ$) among all the investigated conditions.

© 2012 Elsevier Masson SAS. All rights reserved.

1. Introduction

Heat exchangers play significant roles in various industrial fields, such as power generation, air conditioning, and petrochemical industry, etc. Development of heat transfer augmentation has been highlighted for decades, because it could reduce energy consumption, save materials, etc. Researchers have made many contributions to technique development for heat transfer enhancement [1]. Thermal augmentation techniques are usually divided into two categories, i.e., passive technique and active technique, according to whether extra power is needed besides the power for fluid flow. The passive techniques are more widely used in practical application as no extra power is needed. Various tube inserts such as the twisted tapes, conical rings, porous media inserts, etc. [2], fall into this category. Many tube inserts could enhance the heat transfer rate because swirls are generated in tube, which facilitate disturbing thermal boundary layer and intensifying fluid mixing. However, thermal augmentation is often accompanied by the increment of flow resistance. Therefore, enough attention should be paid to the variation of flow resistance in developing thermal augmentation techniques.

Up to now, numerous types of tube inserts have been developed [3]. For example, wire coil inserts are efficient in turbulent thermal augmentation by disturbing the fluid in the viscous sub-layer and log layer near the wall. Twisted tapes are most widely used for thermal augmentation of laminar and turbulent flow, because the inserts can generate spiral flow, which effectively facilitates the mixing of fluid, as well as disturbing thermal boundary layer [4–7]. In addition, twist tapes have other advantages, such as steady performance, simple configuration, easy assembly/disassembly. Based on conventional twisted tapes, developments have been made for better performances, such as segmented twisted tapes [8,9], broken twisted tapes [10], serrated twisted tapes [11], helical screw tapes [12–14], and center-cleared twist tape [15].

Conical ring is another type of tube inserts for heat transfer augmentation. Effects of the pitch and diameter, as well as the arrangement of conical rings were experimentally investigated in turbulent flow. Despite of the substantial increase of the flow resistance, the enhancement efficiency of conical rings could exceed unity [16–18]. Moreover, modifications have been studied for better performances [19–21], for example, cut-out conical rings [19], combination of conical-nozzle and swirl generator [20], combination of conical-ring and twisted-tape [21], etc.

Recently, Eiamsa-ard et al. [22] developed a louvered strip insert. They experimentally investigated the effects of forward and backward arrangements, and inclined angle on the thermo-

* Corresponding author. Tel.: +86 27 87542618; fax: +86 27 87540724.
E-mail addresses: faw@mail.hust.edu.cn, catia315@163.com (A. Fan).

1290-0729/$ – see front matter © 2012 Elsevier Masson SAS. All rights reserved.
http://dx.doi.org/10.1016/j.ijthermalsci.2012.06.013

hydraulic performance of turbulent water flow. The results showed that the performance evaluation criterion (PEC) was around 1.17–1.98 for backward arrangement, and 1.11–1.8, for forward arrangement. More recently, Fan et al. [23] performed a numerical study on the thermo-hydraulic performance of turbulent airflow in a circular tube fitted with louvered strip inserts. The results show that the Nusselt number is augmented by 2.75–4.05 times as that of the smooth tube. The value of performance evaluation criterion (PEC) lies in the range of 1.60–2.05, which demonstrates that the louvered strip insert has a very good overall thermo-hydraulic performance.

In our previous study [24], a conical strip insert was developed for thermal augmentation, and a good thermo-hydraulic performance was shown in the turbulent flow regime. In the present work we are about to investigate its performances in the laminar flow regime through numerical simulation. Main attention will be paid to the effects of some geometrical parameters, such as the slant angle (α), geometry angle (β), dimensionless strip-wall gap (δ/D) and strip pitch (s/D).

2. Numerical modeling

2.1. Physics model

Fig. 1 schematically shows the enhanced circular tube fitted with conical strip inserts. Those strips are uniformly arranged with two strips as a group and connected to a central rod. The inner diameter, D, of the tube is 20 mm. The conical strip is a part of a cone surface, whose dimension is characterized by a geometry angle, β (=30, 45, 60 and 90°). The dimensionless strip-wall gap, δ/D equals to 0.10, 0.15, 0.20 and 0.25. The angle between the conical strip and central rod is defined as slant angle, α (=30, 40 and 50°). The strip pitch is normalized by tube diameter, s/D (=1.5, 2.25 and 3.0). Air at the ambient condition acts as the working fluid. Tube wall thickness is not considered and heat conduction in the central rod is also neglected. Heat conduction in the strips (thickness of 1 mm) and convection heat transfer between the strips and fluid are taken into account. The material of the conical strips is stainless steel.

2.2. Governing equations

The following assumptions are made during the numerical modeling:

1) The strip insert is stiff. Thus, the deformation and vibration are neglected;
2) The flow is stable, fully developed;
3) The fluid is continuous, Newtonian, incompressible, isotropic, and with constant physical properties;
4) The influences of gravity and viscous heating are negligible.

The three-dimension stable incompressible flow and heat transfer model is used for the numerical study. The conservation equations, including continuity, momentum and energy equations in the Cartesian coordinate system are presented below in a tensor form.

Continuity equation:

$$\frac{\partial(\rho u_j)}{\partial x_j} = 0 \tag{1}$$

Momentum equation:

$$\frac{\partial(\rho u_i u_j)}{\partial x_j} = -\frac{\partial p}{\partial x_i} + \frac{\partial}{\partial x_j}\left(\mu\left(\frac{\partial u_i}{\partial x_j} + \frac{\partial u_j}{\partial x_i}\right)\right) \tag{2}$$

Energy equation:

$$\frac{\partial(\rho c_p T u_j)}{\partial x_j} = \frac{\partial}{\partial x_j}\left(\lambda\left(\frac{\partial T}{\partial x_j}\right)\right) \tag{3}$$

where T and p are fluid temperature and pressure, u is fluid velocity vector; ρ and c_p are fluid density and specific heat at constant pressure; λ and μ are thermal conductivity and viscosity, respectively.

2.3. Computation region, mesh and boundary conditions

Under the assumption that the flow is fully developed, and to reduce the computation load, only a quarter of the section between two strips is selected as the computation region and periodic boundary is specified for it. In addition, it also facilitates the comparisons between the thermo-hydraulic performances under different conditions by using the concept of periodic flow boundary. Gambit 2.3, the preprocessor of CFD simulation is used for geometrical modeling and mesh generation. Fig. 2(a) presents the geometrical model and it is meshed with unstructured grids, as shown in Fig. 2(b). Momentum boundaries of all solid walls are of no slip and no penetration. In order to obtain an approximately constant temperature increase of the fluid under different inlet flow velocities, we set the heat flux on the tube wall to be proportional to the Reynolds number.

2.4. Computation scheme and validation

Three dimensional double-precision version of Fluent 6.3 is used as the solver. All above-mentioned equations accompanied by boundary conditions are discretized with finite volume formulation. The momentum and energy terms are treated with the second-order upwind scheme, while the pressure term is treated with standard scheme. Numerical computations are done with pressure-based solver. Pressure and velocity are coupled with the 'SIMPLE' algorithm. The convergent criterions are set as: relative residual of 1E-5 for both continuity and momentum and 1E-8 for energy. Mesh independence was checked by using three sets of grids (100,000, 150,000 and 330,000). The relative difference between the computation results of the latter two was within 3%.

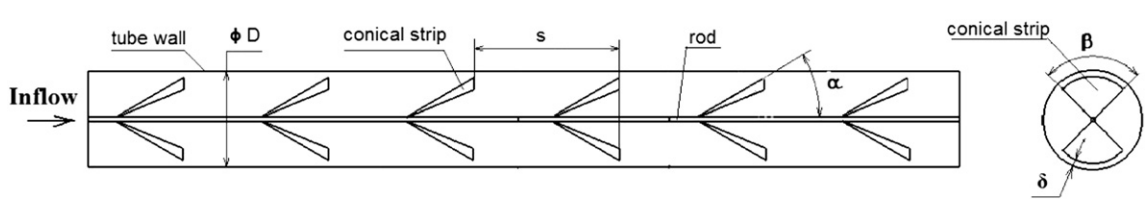

Fig. 1. Schematic of the enhanced tube with conical strip inserts.

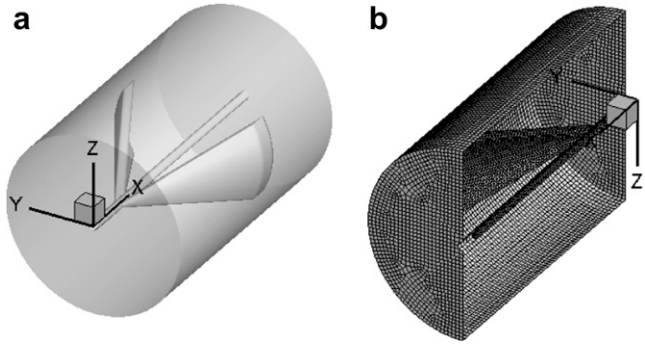

Fig. 2. Mesh generation of a cycle for the enhanced tube with conical strip inserts. (a) Geometrical model and coordinate system; (b) meshes.

Thus the grid system of 150,000 was adopted in the final computations.

To validate the numerical method described above, plain circular tube with a diameter of 20 mm is modeled with uniform heat flux imposed on the wall under laminar flow condition. The computed Nusselt numbers and friction factors are compared with those of the well-known theoretical formulas, i.e., 4.364 and 64/*Re* for Nusselt number and friction factor, respectively. The comparisons are presented in Fig. 3, which demonstrate the computation results are in a good agreement with theoretical values (relative discrepancy within 3%). Therefore, it could be assumed that the present numerical predictions have reasonable accuracy.

In order to find out the critical length for the fully developed flow, computation was made using a full-length tube with 14 pairs of strips at $Re = 900$ as an example [25]. The velocity field is shown in Fig. 4(a), from which it is clearly seen that the flow becomes fully developed after 6–7 pairs of strips from the inlet, and the flow pattern of fully developed flow agrees well with that computed with periodic model in Fig. 4(b). This verifies that periodic flow boundary can be adopted in the computations.

3. Numerical results

3.1. Calculation methods of thermo-hydraulic performances

After the convergence, the fields of velocity, pressure and temperature are obtained, from which thermo-hydraulic performances are calculated, including heat transfer rate, flow resistance and overall thermo-hydraulic performance.

Heat transfer rate is presented in the form of Nusselt number, *Nu*, which is calculated as

$$Nu = \frac{hD}{\lambda} \tag{4}$$

here h is the convective heat transfer coefficient at tube wall and it is calculated as

$$h = \frac{q}{T_{\mathrm{m,w}} - T_{\mathrm{m,f}}} \tag{5}$$

where q is the heat flux of tube wall, $T_{\mathrm{m,w}}$ and $T_{\mathrm{m,f}}$ are the mean temperatures of tube wall and fluid, respectively. In the cylindrical coordinate system, they are calculated as

$$T_{\mathrm{m,w}} = \frac{1}{A}\int_0^A T_{\mathrm{w}} dS \tag{6}$$

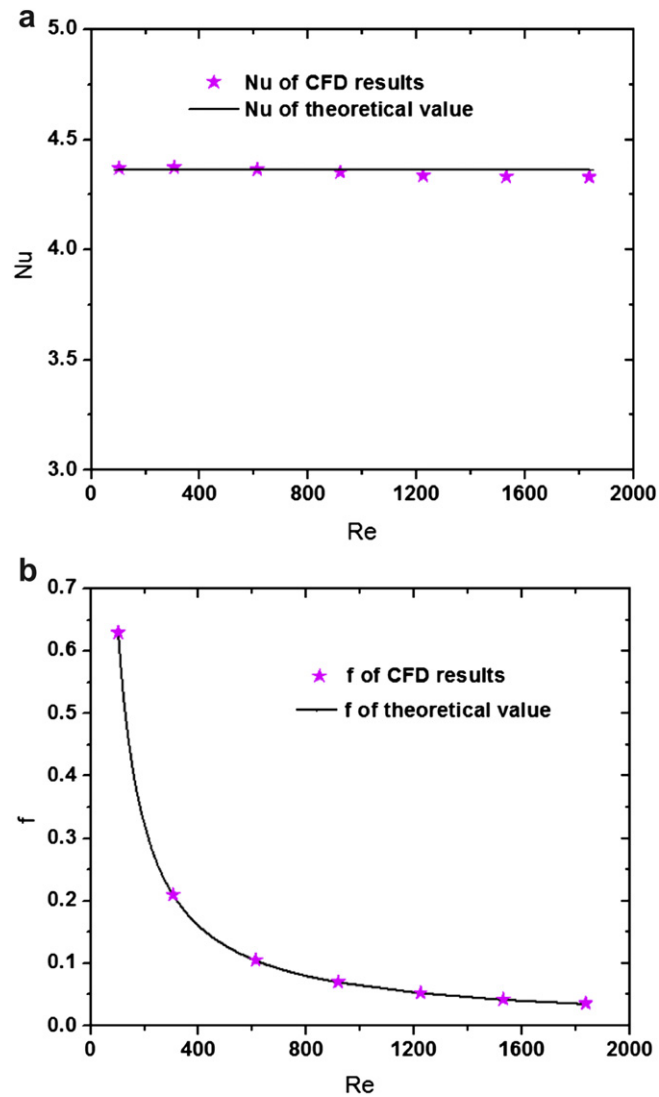

Fig. 3. Comparison between the numerical results and theoretical data of Nusselt number and friction factor of plain tube in the fully developed laminar flow regime: (a) *Nu*, (b) *f*.

$$T_{\mathrm{m,f}} = \frac{\int_0^{D/2} \rho u_{\mathrm{x}} r T_{\mathrm{f}} dr}{\int_0^{D/2} \rho u_{\mathrm{x}} r dr} \tag{7}$$

where T_{w} and T_{f} are the temperatures of tube wall and fluid, respectively. u_{x} is the axial velocity of cross section, and A is the surface area of tube wall, while dS is the micro-element of area. The friction factor, f, is calculated as

$$f = \frac{2\Delta p D}{L \rho u_{\mathrm{m,x}}^2} \tag{8}$$

where $u_{\mathrm{m,x}}$ is the mean axial velocity of cross section, which is calculated as

$$u_{\mathrm{m,x}} = \frac{8}{D^2}\int_0^{D/2} u_{\mathrm{x}} r dr \tag{9}$$

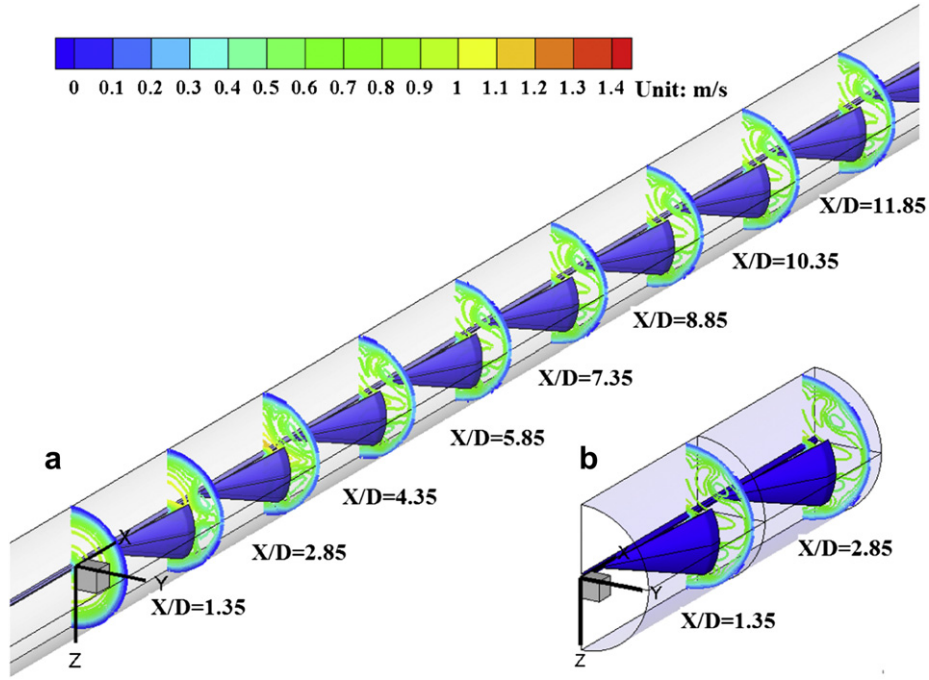

Fig. 4. Contours of X-velocity of different sections at $Re = 900$ for the full-length enhanced tube and periodic model, the dimensionless strip pitch is 1.5. (a) Full-length tube, (b) periodic model.

The widely used performance evaluation criterion (PEC) is adopted here to evaluate the overall thermo-hydraulic performance of the enhanced tube. It is calculated through the following formula [26]

$$\mathrm{PEC} = \frac{Nu/Nu_0}{(f/f_0)^{1/3}} \tag{10}$$

where Nu and f are the Nusselt number and friction factor of the enhanced tube, respectively; while Nu_0 and f_0 are the counterparts of the plain tube at the same Reynolds number, respectively.

The average Nusselt number, friction factor and PEC value are respectively defined as their average values over the whole investigated Reynolds numbers in the current study.

3.2. Variation of the Nusselt number

Fig. 5(a)–(d) demonstrates the effects of slant angle, geometry angle, dimensionless strip-wall gap and pitch on the Nusselt number, respectively. It is noted from Fig. 5 that the parameter combination of $\alpha = 30°$, $\beta = 90°$, $\delta/D = 0.15$ and $s/D = 1.5$ yields the best heat transfer rate, whose average Nusselt number is augmented by around 5.51 times that of the smooth tube. This verifies that the conical strip could enhance heat transfer rate effectively in the laminar flow regime. Moreover, some general tendencies can be drawn from Fig. 5(a)–(d). First, the Nusselt number rises with the increment of the Reynolds number. Second, the Nusselt number rises with the increment of the geometry angle, or with the decrement of dimensionless strip-wall gap or strip pitch when other parameters are fixed. In other words, the larger the geometry angle, or the smaller the dimensionless strip-wall gap or strip pitch, the higher the heat transfer rate is. Thirdly, the impact of the slant angle depends on the magnitude of Reynolds number. When the Reynolds number is above ~500, the Nusselt number of enhanced tube increases with the increment of slant angle, otherwise the trend is opposite.

To facilitate comparing the effects of the slant angle, geometry angle, dimensionless strip-wall gap and pitch on the heat transfer enhancement, all curves in Fig. 5(a)–(d) are put together in Fig. 5(e). From this figure, one can see that thermal performance of the enhanced tube is most sensitive to the geometry angle. For the conical strip with $\alpha = 30°$, $\delta/D = 0.15$ and $s/D = 1.5$, a relatively larger geometry angle has a much better effect on heat transfer enhancement, and the average Nusselt number is about 24.1 at the geometry angle of 90°, which is about 40% larger than that of 30° geometry angle. Moreover, it is also seen that impacts of the strip pitch and strip-wall gap on the Nusselt number are not as significant as that of the geometry angle, but their impacts are relatively larger than that of the slant angle. When the dimensionless strip pitch decreases from 3 to 1.5, or the dimensionless strip-wall gap decreases from 0.25 to 0.1, the average Nusselt number increases by ~30% and 22%, respectively. The impact of the slant angle is relatively weaker, and the average Nusselt number increases by less than 10% when slant angle changes from 30° to 50°.

3.3. Variation of the friction factor

Effects of the slant angle, geometry angle, dimensionless strip-wall gap and pitch on the friction factor f and the ratio f/f_0 are depicted in Fig. 6(a)–(d), respectively. Contrast with the Nusselt number, the friction factor decreases with the increment of the Reynolds number, while the ratio f/f_0 varies in an opposite tendency. Moreover, it is noted from Fig. 6(a)–(d) that for all the investigated cases the average friction factor of the enhanced tube is increased by 5.31–14.77 times that of the plain tube (average $f = 0.59$–1.51). In addition, the friction factor f and the ratio f/f_0 rise with the increment of the slant angle or geometry angle, or with the decrement of dimensionless strip-wall gap or strip pitch of conical strip when the Reynolds number is the same. In other words, the larger the slant angle or geometry angle, or the smaller the dimensionless strip-wall gap or strip pitch, the larger the flow resistance and flow resistance increment (i.e., f/f_0) are.

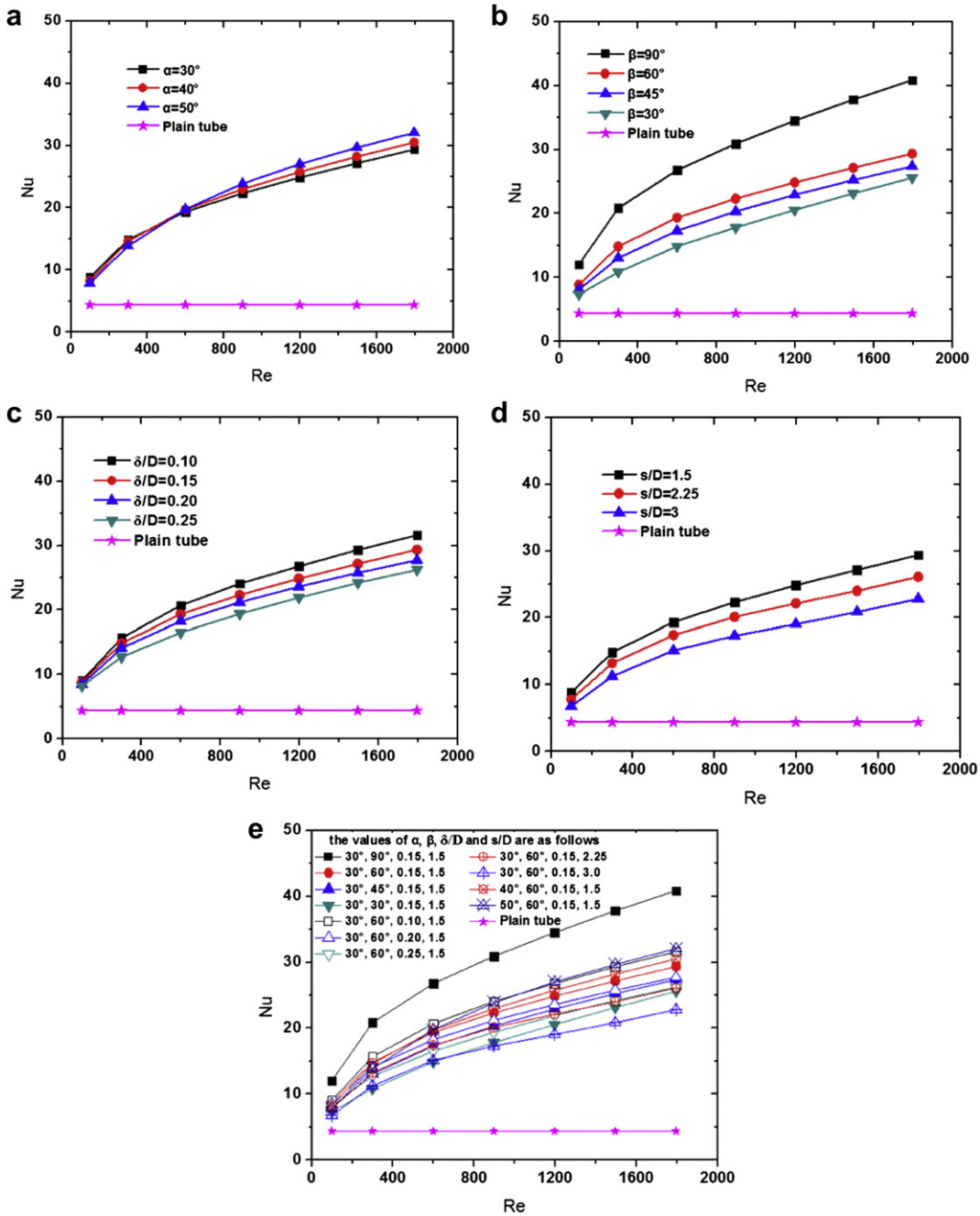

Fig. 5. Variation of the Nusselt number with Reynolds number for different slant angle, geometry angle, dimensionless strip-wall gap and pitch: (a) $\beta = 60°$, $\delta/D = 0.15$, $s/D = 1.5$, (b) $\alpha = 30°$, $\delta/D = 0.15$, $s/D = 1.5$, (c) $\alpha = 30°$, $\beta = 60°$, $s/D = 1.5$, (d) $\alpha = 30°$, $\beta = 60°$, $\delta/D = 0.15$, (e) curve pool.

Similarly, for the convenience of comparing the influence of slant angle, geometry angle, dimensionless strip-wall gap and pitch on the flow resistance, we put all the f and f/f_0 curves of Fig. 6(a)–(d) in Fig. 6(e), (f) respectively. From Fig. 6(e), (f) one can see that the flow resistance of the enhanced tube is most sensitive to the geometry angle, and a relatively larger geometry angle leads to much larger friction factor f and ratio f/f_0. For the conical strip with $\alpha = 30°$, $\delta/D = 0.15$ and $s/D = 1.5$, the average friction factor f and the ratio f/f_0 rise by about 152% and 178% respectively when the geometry angle increases from 30° to 90°. Moreover, impacts of the strip pitch and strip-wall gap on the flow resistance are not as significant as that of the geometry angle, but their impacts are relatively larger than that of the slant angle. The average friction factor f and the ratio f/f_0 increase by 56.8% and 56.7% when the dimensionless strip pitch changes from 3.0 to 1.5. As the dimensionless strip-wall gap is decreased from 0.25 to 0.10, f and f/f_0 increase by 30% and 44.6%. The influence of slant angle is relatively weaker. The variations of average friction factor f and ratio f/f_0 are about 25.6% and 13.5% when slant angle changes from 30° to 50°.

3.4. Variation of the performance evaluation criterion (PEC)

Fig. 7(a)–(d) shows the effect of above-mentioned parameters on the overall thermo-hydraulic performance of the enhanced tube. From this figure it is noted that the overall performance of

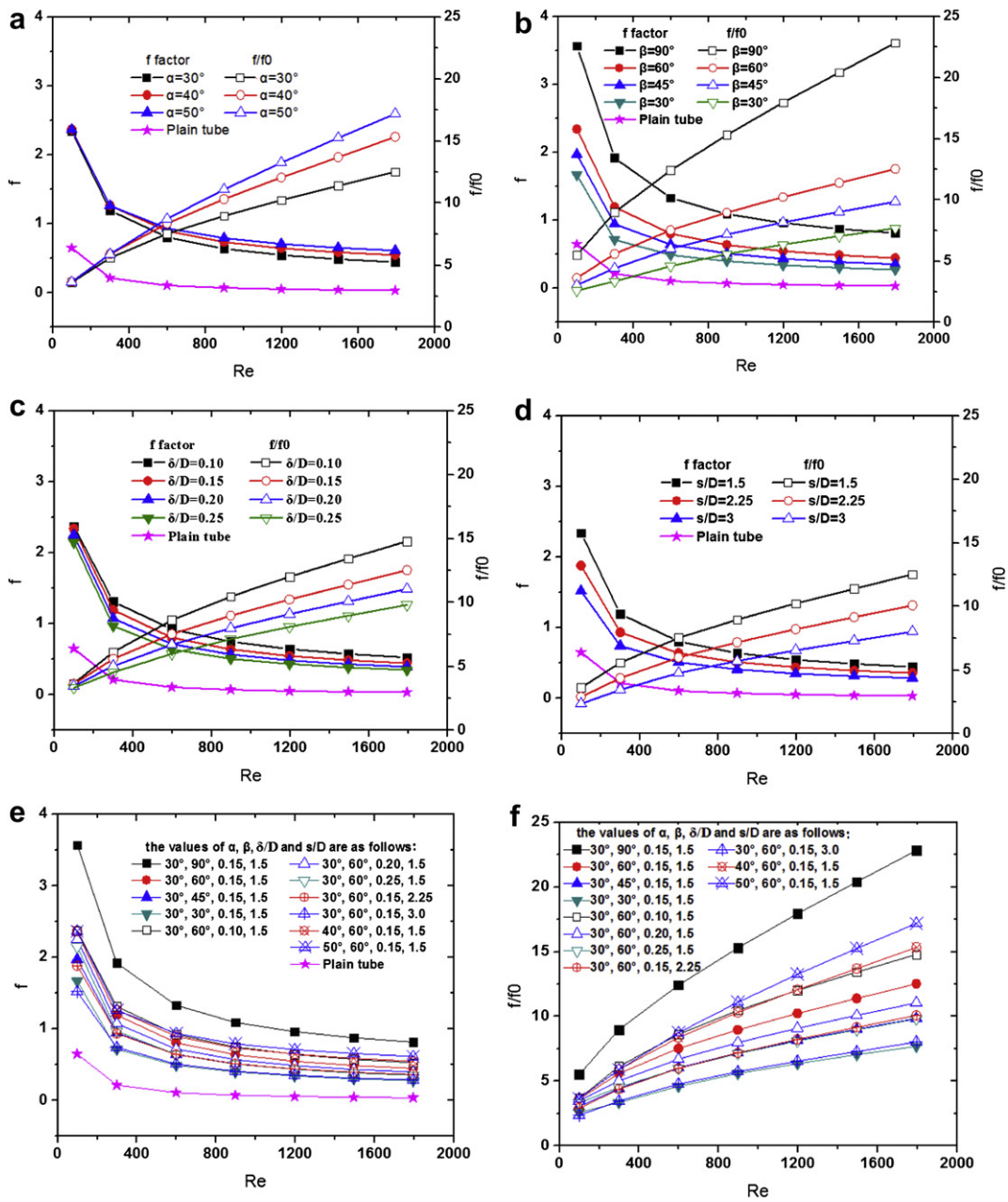

Fig. 6. Variation of the friction factor f and the ratio f/f_0 with Reynolds number for different slant angle, geometry angle, dimensionless strip-wall gap and pitch: (a) $\beta = 60°$, $\delta/D = 0.15$, $s/D = 1.5$, (b) $\alpha = 30°$, $\delta/D = 0.15$, $s/D = 1.5$, (c) $\alpha = 30°$, $\beta = 60°$, $s/D = 1.5$, (d) $\alpha = 30°$, $\beta = 60°$, $\delta/D = 0.15$, (e) f curve pool, (f) f/f_0 curve pool.

enhanced tube increases monotonically with the Reynolds number in laminar flow regime. The PEC value lies in the range of 1.17–2.97, while the average PEC value ranges from 2.08 to 2.37 for all the investigated cases, which demonstrates that the conical strip insert has a good overall thermo-hydraulic performance in the laminar flow regime.

However, as can be seen from the definition of PEC (i.e., Eq. (10)), the value of PEC is proportional to Nu/Nu_0 and inversely proportional to $(f/f_0)^{1/3}$. Thus, the relation between the PEC value and slant angle, geometry angle, strip-wall gap and pitch is very complicated. From Fig. 7(a), it can be seen that the relation between the PEC value and slant angle is relatively weaker and depends on the magnitude of Reynolds number. In brief, among the three slant angles, the case of 30° yields the best average PEC value of 2.32, and the relative variations are within 3% between each other.

From Fig. 7(b), one can see that the impact of the geometry angle on PEC value is relatively larger. The maximum relative variation of average PEC value is about 5% for the four geometry angles. Moreover, it is seen that despite all the PEC values increase with Reynolds number, the PEC gradients of various geometry angles differ a lot and depend on the magnitude of Reynolds numbers. In general, a relatively larger geometry angle facilitates to yield larger PEC value at smaller Reynolds number, while a smaller geometry angle helps to obtain better overall performance at larger Reynolds number. For the whole Reynolds number range of laminar flow, strips with a geometry angle of 60° are more likely to obtain larger PEC value.

It is seen from Fig. 7(c)–(d) that the PEC value rises monotonously with the decrement of dimensionless strip-wall gap and strip pitch. In other words, the smaller the dimensionless strip-wall

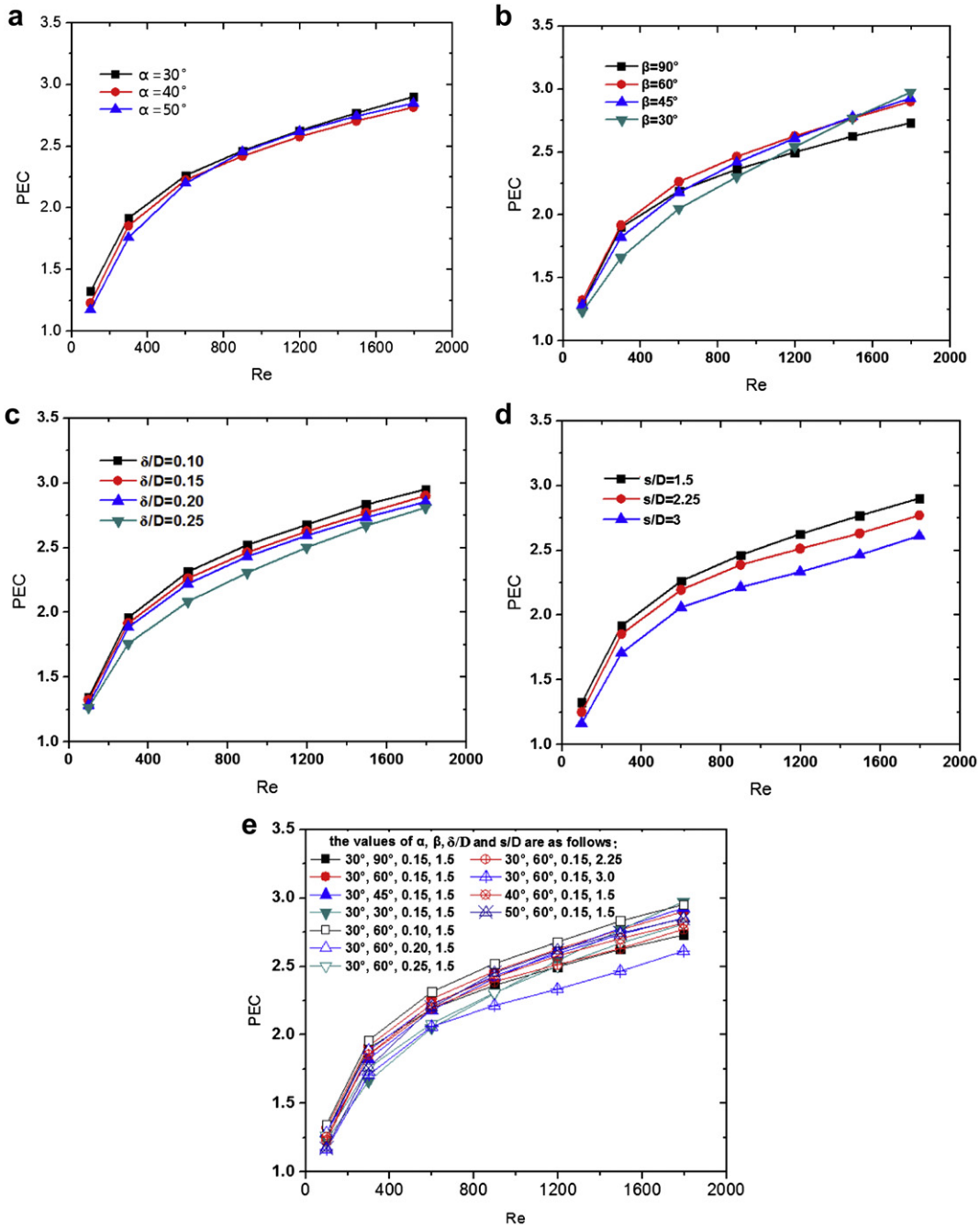

Fig. 7. Variation of the PEC value with Reynolds number for different slant angle, geometry angle, dimensionless strip-wall gap and pitch: (a) $\beta = 60°$, $\delta/D = 0.15$, $s/D = 1.5$, (b) $\alpha = 30°$, $\delta/D = 0.15$, $s/D = 1.5$, (c) $\alpha = 30°$, $\beta = 60°$, $s/D = 1.5$, (d) $\alpha = 30°$, $\beta = 60°$, $\delta/D = 0.15$, (e) curve pool.

gap or strip pitch, the better the overall performance is. Moreover, it is observed from the figure that the maximum relative variation of average PEC value with dimensionless strip-wall gap is about 5.5%, slightly larger than that of geometry angle. The variation of average PEC value with the strip pitch is much more notable. When the dimensionless strip pitch is changed from 3.0 to 1.5, the average PEC value is increased by about 10.5%.

Fig. 7(e) depicts all the data in Fig. 7(a)–(d) for the convenience of comparison. From this figure it is clearly seen that for all the investigated cases, the best parameter combination is $\alpha = 30°$, $\beta = 60°$, $\delta/D = 0.10$ and $s/D = 1.5$, under which the largest average PEC value of 2.37 yields. Moreover, it is observed that larger strip pitch results in lower PEC value at almost all laminar Reynolds number. Smaller geometry angle and larger strip-wall gap should be also avoided at small Reynolds numbers. Furthermore, strips with a larger geometry angle should not be adopted for the application of larger Reynolds number.

4. Discussions

The numerical results demonstrate that the heat transfer rate and flow resistance of enhanced tube are strongly related with the parameter combination of the conical strip inserts. The reason is that these parameters have substantial effects on fluid mixing and

boundary layer disturbing inside the tube. Thus, we present the flow and temperature fields of the cases at $Re = 900$ as examples to discuss the effect of the geometrical parameters.

Fig. 8(a)–(c) and Fig. 9(a)–(c) show the contours of velocity and temperature fields in the longitudinal and horizontal sections of enhanced tube for different slant angles, respectively, while Fig. 8(i) and Fig. 9(i) are the contours of velocity and temperature fields of the plain tube, whose heat flux of tube wall is 1/3 times that of enhanced tube. It is clearly seen from Fig. 8(a)–(c) that the fluid mixing and boundary layer disturbing are greatly intensified by conical strip inserts, and the intensity increases with the increment of slant angle. Thus the flow boundary layer becomes thinner and friction factor increases at larger slant angle, in accordance with what is shown in Fig. 6(a). Meanwhile, as shown in the horizontal sections of Fig. 9(a)–(c), the fluid temperature in core region grows more uniform at larger slant angle, and the temperature gradient near wall becomes larger. As a result, the heat transfer rate increases with slant angle, too.

The effects of dimensionless strip-wall gap on the flow resistance and heat transfer rate are analyzed with the contours of the velocity and temperature fields in the longitudinal and horizontal sections of enhanced tube, as shown in Fig. 8(a), (d), (e), (f) and Fig. 9(a), (d), (e), (f), respectively. It is observed that both the flow and temperature fields are disturbed by the conical strips. Moreover, it could be seen in both the longitudinal and horizontal sections (i.e., Fig. 9(a), (d), (e) and (f)) that as the strip-wall gap is reduced, the thermal boundary layers become thinner by more severe disturbances, and the fluid temperature in core region becomes more uniform. As a result, the heat transfer rate rises. Meanwhile, as can be seen from Fig. 8(a), (d), (e) and (f), with the decrement of strip-wall gap, the flow boundary become thinner, and bulk flow velocity increases due to more blocking area of strips. These will also lead to an increase of the flow resistance.

The contours of velocity and temperature fields in the longitudinal and horizontal sections of enhanced tube are presented in Fig. 8(a), (g), (h) and Fig. 9(a), (g), (h) for different strip pitches, respectively. It is clearly seen that the smaller the distance from the strip, the smaller the disturbance on fluid is. Therefore, with the increment of strip pitch, both the heat transfer rate and flow resistance are decreased.

Fig. 10(a)–(d) and Fig. 11(a)–(d) depict the contours of velocity and temperature fields in the cross section ($X/D = 1.4$) of enhanced tube at $Re = 900$ for different geometry angle, while Fig. 10(e) and Fig. 11(e) show the corresponding contours of plain tube. It's clearly seen that both the flow and temperature fields of enhanced tube are intensively disturbed by conical strip inserts. With the increment of geometry angle, the disturbed region expands, and the temperature field becomes more uniform in core region. Thus, the

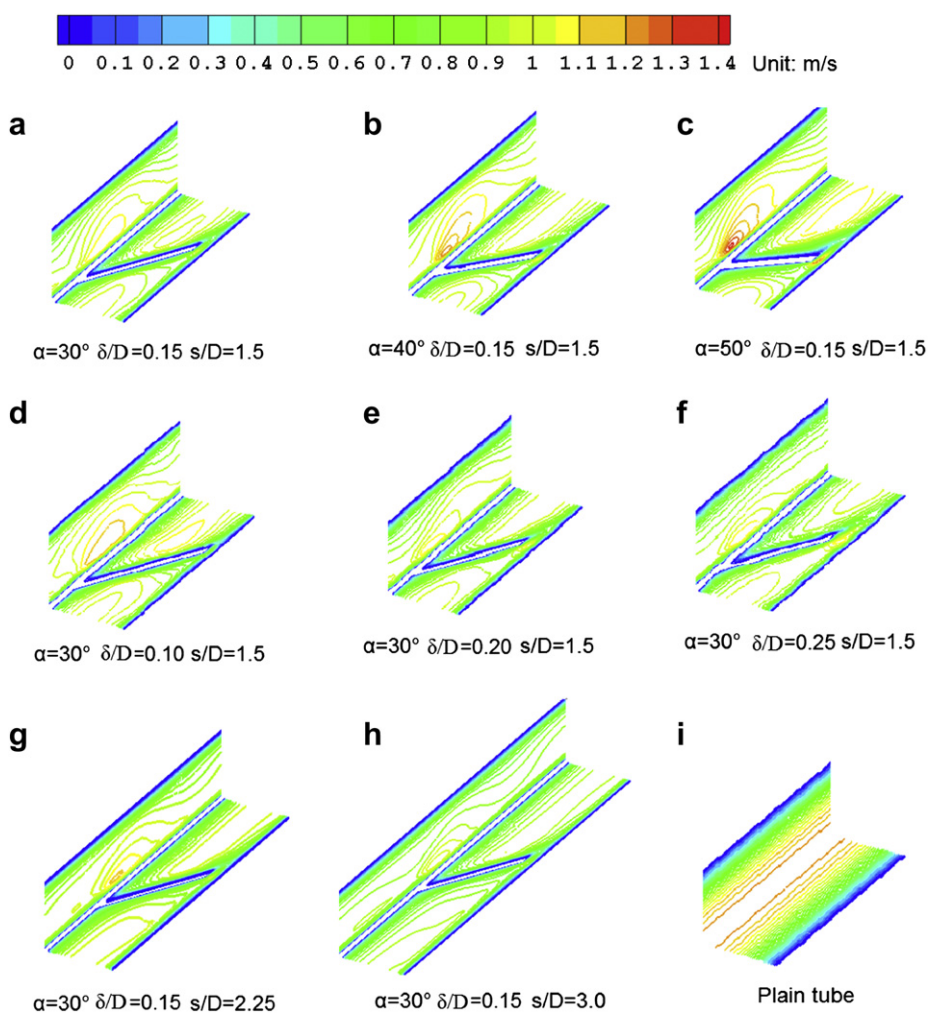

Fig. 8. Contours of velocity magnitude in the longitudinal and horizontal sections at $Re = 900$ for different slant angle, dimensionless strip-wall gap and pitch. The geometry angle of conical strips is 60°.

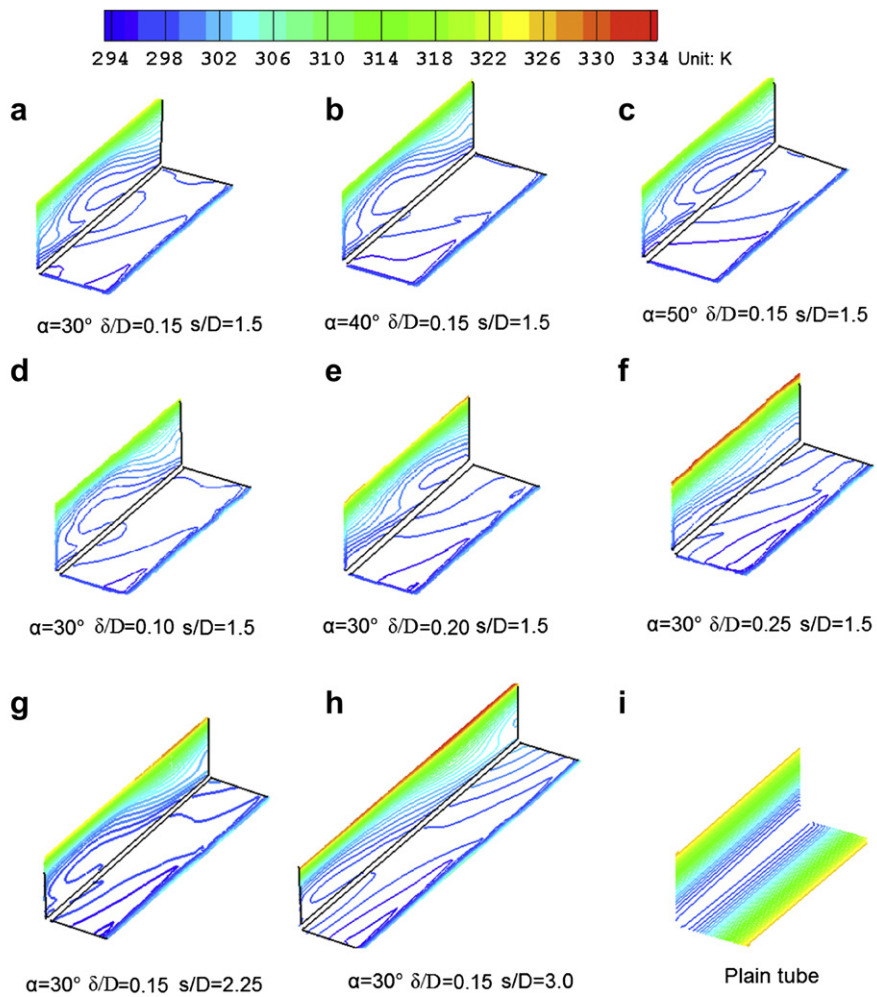

Fig. 9. Contours of temperature in the longitudinal and horizontal sections at $Re = 900$ for different slant angle, dimensionless strip-wall gap and pitch. The geometry angle of conical strips is 60°.

heat transfer rate increases. As a result, the temperature of tube wall is decreased, as shown in Fig. 11(a)–(d). At the same time, the flow resistance rises as well.

The overall performance of the enhanced tube, which is characterized by the PEC value, is determined by the Nusselt numbers and friction factors before and after the thermal augmentation. The relation between PEC value and geometrical parameters is much more complicated. For instance, larger geometry angle and smaller dimensionless strip-wall gap and pitch can effectively enhance the heat transfer rate, however they could also increase the flow resistance. Too large geometry angle results in good heat transfer rate, but the PEC value is not large because flow resistance is considerably increased. Too small geometry angle has high PEC value at large Reynolds number, however, it behaves badly at low Reynolds numbers because of the small heat transfer rate. Larger strip pitch and strip-wall gap facilitate lower flow resistance, however, they yield lower overall performance due to small heat transfer rate. In summary, for all the investigated cases, the

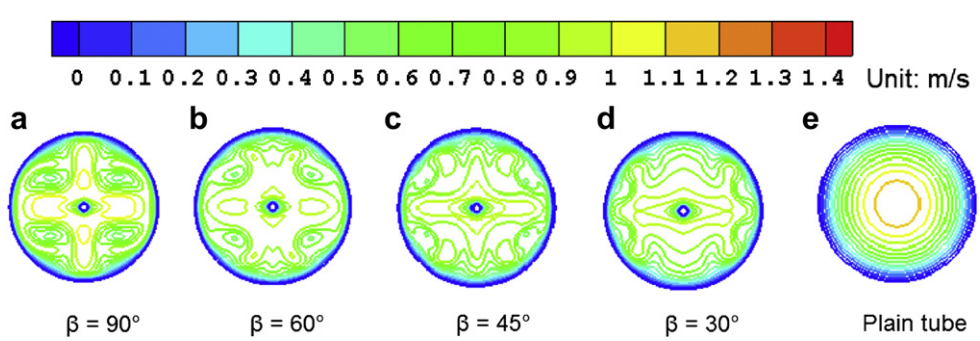

Fig. 10. Contours of velocity magnitude in the cross section of $X/D = 1.4$ at $Re = 900$ for different geometry angles. The slant angle, dimensionless strip-wall gap and pitch are 30°, 0.15 and 1.5, respectively.

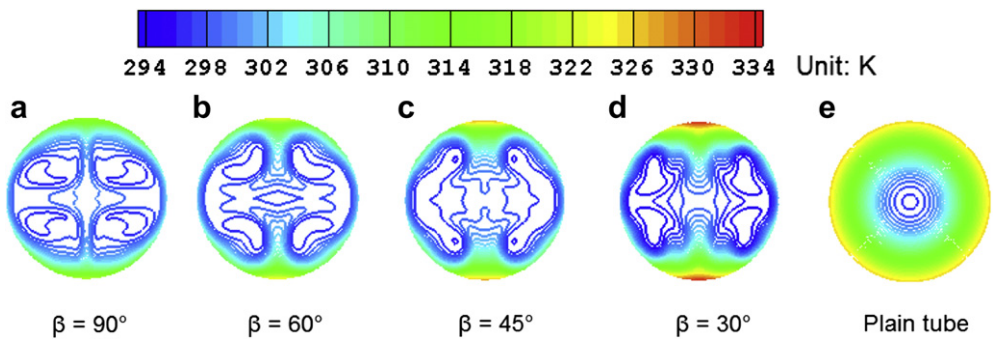

Fig. 11. Contours of temperature in the cross section of $X/D = 1.4$ at $Re = 900$ for different geometry angles. The slant angle, dimensionless strip-wall gap and pitch are 30°, 0.15 and 1.5, respectively.

parameter combination of small slant angle, dimensionless strip-wall gap and pitch, as well as moderate geometry angle, i.e., $\alpha = 30°$, $\beta = 60°$, $\delta/D = 0.10$ and $s/D = 1.5$, yields the best overall performance over the whole investigated Reynolds numbers range.

5. Conclusions

Conical strip inserts were studied for the laminar thermal augmentation in a circular tube in the present study. Variations of the Nusselt number, friction factor, and performance evaluation criteria (PEC) with the slant angle, geometry angle, strip-wall gap and strip pitch were obtained through numerical methods. Computation results show the average friction factor of enhanced tube is increased by 5.31–14.77 times (average $f = 0.59–1.51$), while the average Nusselt number is augmented by 3.70–5.51 times (average $Nu = 16.15–24.05$) that of the plain tube. The average PEC value lies in the range of 2.08–2.37. Numerical results indicate that larger geometry angle, or smaller strip-wall gap, or smaller strip pitch can effectively enhance the heat transfer rate, but also increase the flow resistance. The impact of slant angle depends on the magnitude of Reynolds number. Moreover, it is shown the heat transfer rate and flow resistance of enhanced tube are most sensitive to the geometry angle. The influences of dimensionless strip-wall gap and pitch are secondary, and the slant angle is the weakest factor. The PEC value rises monotonically with the increment of Reynolds number. It is most sensitive to the strip pitch, while the impact of slant angle is the weakest. In brief, relatively high PEC value can be obtained by the parameter combination of small slant angle, strip-wall gap and strip pitch, as well as moderate geometry angle ($\delta/D = 0.10$, $\alpha = 30°$, $s/D = 1.5$, $\beta = 60°$) over the whole investigated Reynolds numbers.

Acknowledgments

This work was supported by the Natural Science Foundations of China (Nos. 51036003, 51076054 and 51076057).

References

[1] A.E. Bergles, ExHFT for fourth generation heat transfer technology, Exp. Therm. Fluid Sci. 26 (2002) 335–344.
[2] V. Zimparov, Energy conservation through heat transfer enhancement techniques, Int. J. Energy Res. 26 (2002) 675–696.
[3] L. Wang, B. Sunden, Performance comparison of some tube inserts, Int. Commun. Heat Mass 29 (2002) 45–56.
[4] P. Naphon, Heat transfer and pressure drop in the horizontal double pipes with and without twisted tape insert, Int. Commun. Heat Mass 33 (2006) 166–175.
[5] R.M. Manglik, A.E. Bergles, Heat transfer and pressure drop correlations for twisted tape inserts in isothermal tubes: part I laminar flows, J. Heat Transfer 115 (1993) 881–889.
[6] R.M. Manglik, A.E. Bergles, Heat transfer and pressure drop correlations for twisted tape inserts in isothermal tubes: part II transition and turbulent flows, J. Heat Transfer 115 (1993) 890–896.
[7] A. Kumar, B.N. Prasad, Investigation of twisted tape inserted solar water heaters – heat transfer, friction factor and thermal performance results, Renew. Energy 19 (2000) 379–398.
[8] S.K. Saha, A. Dutta, S.K. Dhal, Friction and heat transfer characteristics of laminar swirl flow through a circular tube fitted with regularly spaced twisted-tape elements, Int. J. Heat Mass Transf. 44 (2001) 4211–4223.
[9] S. Eiamsa-ard, C. Thianpong, P. Promvonge, Experimental investigation of heat transfer and flow friction in a circular tube fitted with regularly spaced twisted tape elements, Int. Commun. Heat Mass 33 (2006) 1225–1233.
[10] S.W. Chang, T.L. Yang, J.S. Liou, Heat transfer and pressure drop in tube with broken twisted tape insert, Exp. Therm. Fluid Sci. 32 (2007) 489–501.
[11] S.W. Chang, Y.J. Jan, J.S. Liou, Turbulent heat transfer and pressure drop in tube fitted with serrated twisted tape, Int. J. Therm. Sci. 46 (2007) 506–518.
[12] P. Sivashanmugam, S. Suresh, Experimental studies on heat transfer and friction factor characteristics of laminar flow through a circular tube fitted with helical screw-tape inserts, Appl. Therm. Eng. 26 (2006) 1990–1997.
[13] P. Sivashanmugam, S. Suresh, Experimental studies on heat transfer and friction factor characteristics of turbulent flow through a circular tube fitted with regularly spaced helical screw-tape inserts, Appl. Therm. Eng. 27 (2007) 1311–1319.
[14] S. Eiamsa-ard, P. Promvonge, Enhancement of heat transfer in a tube with regularly-spaced helical tape swirl generators, Sol. Energy 78 (2005) 483–494.
[15] J. Guo, A.W. Fan, X.Y. Zhang, W. Liu, A numerical study on heat transfer and friction factor characteristics of laminar flow in a circular tube fitted with center-cleared twisted tape, Int. J. Therm. Sci. 50 (2011) 1263–1270.
[16] K. Yakut, B. Sahin, Flow-induced vibration analysis of conical rings used for heat transfer enhancement in heat exchangers, Appl. Energy 78 (2004) 273–288.
[17] K. Yakut, B. Sahin, C. Celik, S. Canbazoglu, Performance and flow-induced vibration characteristics for conical-ring turbulators, Appl. Energy 79 (2004) 65–76.
[18] P. Promvonge, Heat transfer behaviors in round tube with conical ring inserts, Energy Convers. Manage. 49 (2008) 8–15.
[19] A. Durmus, Heat transfer and exergy loss in cut out conical turbulators, Energy Convers. Manage. 45 (2004) 785–796.
[20] P. Promvonge, S. Eiamsa-ard, Heat transfer enhancement in a tube with combined conical-nozzle inserts and swirl generator, Energy Convers. Manage. 47 (2006) 2867–2882.
[21] P. Promvonge, S. Eiamsa-ard, Heat transfer behaviors in a tube with combined conical-ring and twisted-tape insert, Int. Commun. Heat Mass 34 (2007) 849–859.
[22] S. Eiamsa-ard, S. Pethkool, C. Thianpong, P. Promvonge, Turbulent flow heat transfer and pressure loss in a double pipe heat exchanger with louvered strip inserts, Int. Commun. Heat Mass 35 (2008) 120–129.
[23] A. Fan, J. Deng, A. Nakayama, W. Liu, Parametric study on turbulent heat transfer and flow characteristics in a circular tube fitted with louvered strip inserts, Int. J. Heat Mass Transf 55 (2012) 5205–5213.
[24] A.W. Fan, J.J. Deng, J. Guo, W. Liu, A numerical study on thermo-hydraulic characteristics of turbulent flow in a circular tube fitted with conical strip inserts, Appl. Therm. Eng. 31 (2011) 2819–2828.
[25] P. Promvonge, W. Jedsadaratanachai, S. Kwankaomeng, C. Thianpong, 3D simulation of laminar flow and heat transfer in V-baffled square channel, Int. Commun. Heat Mass 39 (2012) 85–93.
[26] R.L. Webb, Performance evaluation criteria for use of enhanced heat transfer surfaces in heat exchanger design, Int. J. Heat Mass Transf. 24 (1981) 715–726.